*Journal of Thermal Analysis and Calorimetry, Vol. 59 (2000) 699–709*

# MELT BEHAVIOUR OF POLY(*p*-XYLYLENE) (PPX) COATED GEL-SPUN UHMW-PE FIBERS AS REVEALED BY TEMPERATURE MODULATED DSC

*U. Göschel*[*] *and G. W. H. Höhne*

Eindhoven Polymer Laboratories (EPL), Eindhoven University of Technology, Den Dolech 2
P.O. Box 513, NL-5600 MB Eindhoven, The Netherlands

(Received January 14, 1999; in revised form November 9, 1999)

## Abstract

The method of temperature modulated DSC has been applied to obtain additional information about the effect of constraints on the melting behaviour of gel-spun ultra high molecular mass polyethylene (UHMW-PE) fibers coated with a high temperature stable poly(*p*-xylylene) (PPX) polymer. The underlying signal, corresponding to the normal DSC signal, reveals two endothermic peaks for the coated PE fibers. A shift in the underlying and magnitude signal from 142 to 145°C at 0.1 K $\text{min}^{-1}$, a relative small magnitude signal, together with a vanishing step-like change in the phase signal with increasing PPX coating layer thickness characterize the constraints in terms of a hindrance of the melting of the unconstrained orthorhombic crystal fraction. The time constant of the melting process can be estimated as larger than the reciprocal angular frequency $1/\omega=5$ s of the modulation.

**Keywords:** constraints, gel-spun UHMW-PE fibers, hindrance of endothermic transitions, melting behaviour, poly(*p*-xylylene) (PPX) coating, temperature modulated DSC

## Introduction

Due to its low creep resistance, the application of gel-spun UHMW-PE fibers in structural composites is limited [1]. The weak van der Waals interaction between the PE chains enhances the drawability to achieve chain-extended structures. However, at elevated temperatures a strong creep cannot be prevented because of low intermolecular forces. The crystallites themselves are temperature stable but do not represent a sufficient lock-in mechanism to conserve the overall chain extension at higher temperatures.

The question arises whether it is possible to impede the transformation from extended to chain-folded configuration by means of coating with a semi-stiff polymeric material. It is proposed that a suitable polymer jacket will hinder conformational

---

[*] Current address: Department of Polymer Physics and Plastography, Institute of Polymer Testing and Polymer Science (IKP), University of Stuttgart, P.O. Box 801140, D-70511, Stuttgart-Vaihingen; Pfaffenwaldring 32, D-70569, Stuttgart-Vaihingen, Germany

*1418–2874/2000/ $ 5.00*

*Akadémiai Kiadó, Budapest*
*Kluwer Academic Publishers, Dordrecht*

changes due to geometrical reasons. Furthermore, an additional effect on the structural stability might be considered by forming a coating/PE - interface based on epitaxial growth of the coating layer.

Gel-spun UHMW-PE fibers are reported to have a highly oriented and fully chain-extended structure with relatively large and perfect crystalline domains. Pennings and Zwijnenburg [2] described a predominantly orthorhombic crystalline structure with a very low non-crystalline content at room temperature.

Depending on thermal and mechanical conditions different structural transformations are observed. Among them is the transition from an orthorhombic crystal phase to a hexagonal phase associated with a solid-state phase transition, which usually is observed under elevated hydrostatic pressure or constrained conditions [2–4]. Calorimetrical investigations (DSC and DTA) have shown multiple endothermic peaks. It is well-documented that the peak position and enthalpy are strongly affected by the applied constraints [2, 5]. In the case of solution-crystallized UHMW-PE fiber a peak maximum is found to be close to 145°C, e.g. van Mele and Verdonck [5], van Aerle and Lemstra [6] and Pennings and Zwijnenberg [2] using a DSC heating rate of 10 K $\text{min}^{-1}$. It is found that a lower heating rate shifts the peak towards a lower temperature. Own results reveal e.g. a peak maximum at 142.3°C for a heating rate of 2.5 K $\text{min}^{-1}$. The peak described previously coincides with the melting of the chain-extended fraction of the crystalline orthorhombic PE phase. In comparison, the chain-folded fraction shows a melting peak with a maximum at temperatures as low as 134°C. Such a chain-folded morphology is known for a melt-crystallized PE.

The chain-extended fraction of the crystalline orthorhombic PE phase, which does not melt under constrained conditions at 145°C is characterized by two endothermic peaks at 154 and 157°C at a rate of 10 K $\text{min}^{-1}$ and which are attributed to a solid–solid phase transition from the orthorhombic to the hexagonal phase (o–h phase transition) and the melting of the hexagonal phase, respectively [5, 6].

The hexagonal phase in PE was identified as conformationally disordered, denoted as condis phase (Wunderlich and Grebowicz [7]). Such a condis phase is different from a 'normal' hexagonal phase. Essential is that the conformations are locally mobile and disordered, which leads to the possibility of easier diffusion along the chain direction as needed for chain extension (Wunderlich [8]). The hexagonal crystal shows an anomalously high longitudinal mobility of the polymer chains (Bassett *et al.* [9]).

Hsieh and Hu [10] verified the o–h phase transition by means of lattice spacings from wide angle X-ray studies and discussed the much larger thermal expansion coefficient in a-direction ($2.7\cdot10^{-4}$ $\text{K}^{-1}$) in comparison to the b-direction ($6.1\cdot10^{-6}$ $\text{K}^{-1}$) as structural reason.

Constraints can occur as a result of the sample preparation, such as winding, packing in the DSC pan, elevated hydrostatic pressure, impregnating or coating. Despite changes of peak position and area, a fixed value for the ratio of the 154 and 157°C peak enthalpies is described. Smook and Pennings [11] reported about a ratio of 2.5 while van Mele and Verdonck [5] found a value of 2.8 determined from a straight extrapolation from valleys in the endothermic signal to the baseline. Using a different method, that is a deconvolution procedure by means of a peak separation, a ratio of 16 to 9 for the o–h phase transition compared to the melting of the hexagonal phase can be obtained [12]. The three possible endothermic peaks in gel-spun PE as mentioned above are positioned on top of a very broad melting curve which relates to a hindered melting of the chain-extended structure.

Van Aerle and Lemstra [6] embedded ultra-drawn gel-spun UHMW-PE fibers in an epoxy matrix and have described an o–h phase transition at about 153°C. Furthermore, UHMW-PE fiber/epoxy matrix composites have been studied by van Mele and Verdonck [5] to demonstrate that the effect of mechanical constraints on fiber melting increases with fiber thickness and matrix stiffness.

In the present study, a PPX/UHMW-PE composite is chosen which consists of a thin poly (*p*-xylylene) (PPX) polymer coating layer on a commercial gel-spun UHMW-PE fiber. As coating technique the chemical vapor deposition (CVD) process according to Gorham's method has been used [13]. PPX ($–CH_2–C_6H_4–CH_2–$) with a degree of crystallinity up to 60 % can be regarded as mechanically robust and highly temperature stable having a tensile modulus of 2.4 GPa and a melting temperature of about 420°C, respectively [14].

DSC measurements on pure PPX, as polymerized in the crystalline monoclinic $\alpha$-form, show a glass transition (65°C), two crystallization regions (80, 125–200°C) and a melting of oligomers (130–144°C), all are minor changes which are hardly seen in the DSC curve (Wunderlich and coworkers [15]). Furthermore, two different phase transitions are known (Isoda *et al.* [16]); an endothermic, irreversible crystalline $\alpha\rightarrow\beta_1$ phase transition (230–242°C) and an endothermic reversible crystalline $\beta_1\rightarrow\beta_2$ phase transition (260–292°C) [15]. Consequently, there is almost no change in the respective heat flow rate curve of PPX in the temperature range from 100 to 200°C, which includes the melting region of UHMW-PE fibers.

Van der Werff and Pennings [17, 18] have compared UHMW-PE and PPX fibers in their relaxation behaviour at 60% of the load at break. Significant differences are seen in the strain-time curve during a creep and in the stress-time curve during a stress relaxation experiment. PPX reveals almost no change in strain and stress with time whereas UHMW-PE relaxes over 75% of the initial stress during 17.4 h at room temperature.

The present paper aims to elucidate the melting behaviour of PPX coated gel-spun UHMW-PE fibers by means of temperature modulated DSC measurements to obtain additional information in particular on time-dependent processes during transitions.

## Experimental

### *Sample preparation*

A commercial ultra-drawn gel-spun Stamylan UHMW-PE fiber grade, provided by DSM Geleen, The Netherlands, were coated with a poly(p-xylylene) (PPX) polymer (Fig. 1) by means of a chemical vapor deposition (CVD) process as described by us in

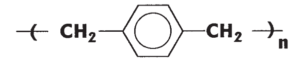

**Fig. 1** Repeating unit structure of poly(*p*-xylylene) (PPX) polymer

[19]. The UHMW-PE fiber substrate used in the present study is characterized by a high molar mass $M_w$≈2.5· $10^6$ g $mol^{-1}$, $M_w/M_n$=4–5 and almost no branching with <$10^{-3}$/$CH_2$. The molecular orientation and order are high, represented by a draw ratio of about 40–50 and a degree of crystallinity of about 80%, respectively [20] (Table 1).

**Table 1** Characteristics of the initial gel-spun UHMW-PE fiber

| Parameter | |
|---|---|
| Fiber titer/dtex | 110 |
| Number of filaments | 95 |
| Density/g $cm^{-3}$ | 0.97 |
| Draw ratio λ | 40–50 |
| E-modulus/GPa | 95 |
| Elongation at break/% | 3.6 |
| Crystallinty/% | 80 |

The PPX layer was deposited on the as-spun and ultradrawn UHMW-PE fiber at a temperature close to 25°C and a vacuum of about 0.02 mbar. The CVD process can be subdivided in three steps; (1) the evaporation of the powdered di-*p*-xylylene dimer, (2) the pyrolysis to form the gaseous p-xylylene monomers and finally (3) the deposition of poly(*p*-xylylene) (PPX) polymer by epitaxial synthesis with simultaneous or successive polymerization and crystallization. Using different values of sublimation temperature ($T_{su}$) and deposition time ($t_{de}$) at the pyrolysis temperature $T_{py}$ = 630°C, a PPX layer thickness of 45 and 320 nm was prepared on the UHMW-PE fiber surfaces (Table 2).

**Table 2** Sample preparation

| Sample | CVD conditions | Coating layer thickness d/nm |
|---|---|---|
| UHMW-PE fiber (PE) | Inital fiber | – |
| PPX coated UHMW-PE filament (PE/PPX-45) | $T_{su}$=130°C, $t_{de}$=45 min | 45 |
| PPX coated UHMW-PE filament (PE/PPX-320 | $T_{su}$=80°C, $t_{de}$=360 min | 320 |

### *Scanning Electron Microscopy (SEM)*

The surface of an as-spun UHMW-PE filament as well as a PPX deposited PE filament was investigated by means of a Cambridge Stereoscan 200 microscope, operating at 20 kV. The micrographs were made of surfaces glued on adhesive tapes and subsequent coated with a gold/palladium layer.

### *Temperature modulated Differential Scanning Calorimetry (TMDSC)*

These measurements were performed on a commercial power compensated DSC (Perkin Elmer DSC-7) which was modified by adding a sinusoidal voltage (from a

Hewlett-Packard wave-form generator) to the set value of the temperature signal in the DSC. This way it was possible to perform temperature-modulated measurements with the program temperature:

$$T(t)=T_o+\beta t+T_a\sin(\omega t) \tag{1}$$

with $\beta$ the underlying heating rate, $T_a$ the temperature amplitude and $\omega=2\pi\nu$ the angular frequency of the modulation. The measured heat flow rate then reads:

$$\Phi(t)=\Phi_u(t)+\Phi_a\cos(\omega t+\varphi) \tag{2}$$

where $\Phi_u$ the underlying heat flow rate (the normal DSC signal), $\Phi_a$ the magnitude (absolute value) and $\varphi$ the phase of the modulated part of the heat flow rate signal. The latter quantities contains components both from the apparatus (caused by the heat flow pathway) and the sample processes, which can be separated from one another, however, not always easily. In general, the real quantities $\Phi_a$ and $\varphi$ are part of the complex quantity $\Phi^*=\Phi_a\exp(-i\varphi)=\Phi'-i\Phi''$, the modulated component of the heat flow rate function.

From the measured heat flow rate function the underlying ($\Phi_u(t)$) and the periodic part was determined as usual. From the latter, the real quantities $\Phi_a$ and $\varphi$ (or $\Phi'$ and $\Phi''$) can be determined in different ways. We have given preference to the method from phase sensitive rectification techniques used in lock-in amplifiers, described elsewhere (Höhne [21]). From $\Phi_a$ and $\varphi$, corrected for apparative influences, it is possible to calculate sample quantities like the (static) heat capacity or, in the case of time dependent processes, the complex heat capacity.

With this tool we performed TMDSC measurements using the original UHMW-PE fiber described above as well as two fibers which were coated with the PPX polymer. A small fiber bundle was cut to a suitable length (mass: 5–6 mg) and put into the normal DSC aluminum pan. We used an underlying heating rate $\beta$=0.1 K min$^{-1}$, a modulation period of 32 s ($\omega$=0.2 rad s$^{-1}$) and a temperature amplitude $T_a$=25 mK (heating-cooling mode). Calculations were done by means of the MAPLE software.

## Results

The gel-spun UHMW-PE fibers were deposited at about 25°C which means a minimal thermal loading. Free shrinkage during deposition was allowed, however, the low deposition temperature is not expected to cause any significant dimension changes.

The PPX coated UHMW-PE fibers were analyzed by means of SEM to examine the uniformity of the coating layers. Figure 2 shows an uncoated UHMW-PE filament whereas Fig. 3 represents a smooth and uniformly deposited PPX layer on the PE filament surface. The coated layer thickness is about 320 nm and corresponds to a ratio of deposited-to-total filament cross-section of about 3.2%. With respect to e.g. Isoda [22], the PPX layer formation from gaseous monomers on substrates can be assumed as epitaxial growth.

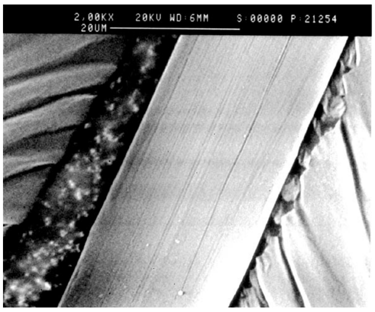

**Fig. 2** SEM micrograph of the initial gel-spun UHMW-PE filament. The magnification is 2000

**Fig. 3** SEM micrograph of a PPX coated UHMW-PE filament. The PPX layer thickness is about 320 nm. The magnification is 2000

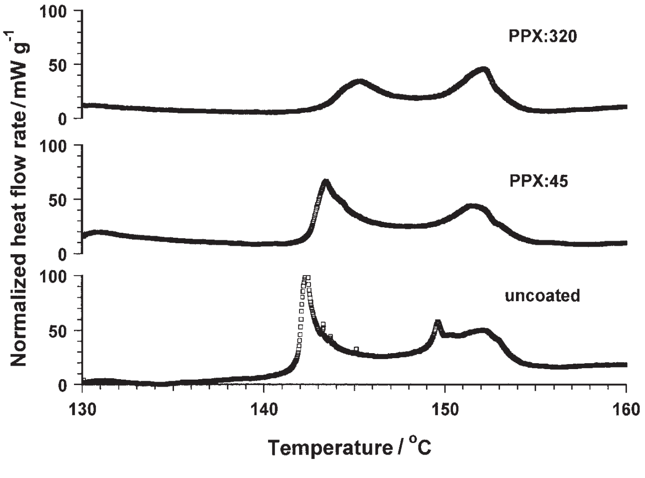

**Fig. 4** Underlying signal ($\Phi_u$) (corresponds to the normal DSC signal) during melting of the initial gel-spun UHMW-PE fiber, UHMW-PE fiber with a 45 nm PPX coating layer and UHMW-PE fiber with a 320 nm PPX coating layer. Heating rate: 0.1 K min$^{-1}$

The results from TMDSC measurements are shown in Figs 4–6. Each figure represents the melting behaviour of the three materials using the curves of the underlying heat flow rate $\Phi_u$ (normal DSC signal) (Fig. 4), the magnitude $\Phi_a$ (Fig. 5) and the phase shift $\varphi$ (Fig. 6) respectively. The curves in Figs 4 and 5 have, for comparison reasons, been normalized due to the mass in question. The interpretation of TMDSC measurements in the melting region is still in scientific discussion. Magnitude and phase are largely influenced by heat transport to the sample, which increases up to 50 times (!) in the melting region (Höhne [23]). Even in the case of no time-dependent processes this leads formally to a complex amplitude of the modulated part of the heat flow rate function. However, it is possible to get some new insights in the melting behaviour of the fiber material from these measurements, which will be explained in the following.

### *Underlying signal*

The underlying signal of the initial (uncoated) gel-spun UHMW-PE fiber reveals three endothermic peaks at 142.4, 149.6 and 152°C at a heating rate of 0.1 K $\text{min}^{-1}$ (Fig. 4) which coincides with the melting of the chain-extended fraction of the crystalline orthorhombic PE phase, the o–h phase transition of the unmolten constrained fraction and the melting of the hexagonal phase, respectively, as reported in literature [5, 6]. From the peak area of the first peak (142.4°C) compared to the total heat of transformation from the fibers to melt (total peak area: 250 J $\text{g}^{-1}$), it can be estimated that a portion of about 35% melts as (chain-extended) orthorhombic phase. The remaining 65% yields the endothermic peaks at 149.6 and 152°C, which is attributed to the effect of constraints hindering the melting of a certain fraction at 142°C. The second (small) peak at 150°C indicates the o–h phase transition of a few percent of unmolten (constrained) material. The third peak represents the melting of the pseudo-hexagonal fraction. The existence of the endothermic peaks in the underlying curve and the corresponding temperatures are in agreement with those in [2, 5] taking the very low heating rate of 0.1 K $\text{min}^{-1}$ into account, which can be regarded as annealing the sample during the run.

The PPX coated UHMW-PE fibers reveal only two endothermic peaks with the maxima at 143.5 and 151.4°C for a PPX layer thickness of 45 nm as well as at 145.3 and 152.1°C for a layer thickness of 320 nm (Table 3). Obviously, both peaks shift towards a higher temperature with increasing PPX layer thickness. The observation of only two high temperature endothermic peaks for the PPX deposited UHMW-PE fiber can be discussed in relation with constraints due to the PPX coating layer. Van Mele and Verdonck [5] analyzed the effect of constraints on the melting behaviour of UHMW-PE as a consequence of a fixation of the fiber around a frame as well as an embedding of the PE in a stiff epoxy matrix system. With respect to their results, we can conclude an increase in constraints with coating layer thickness (0→45→320 nm), which is visible by a shift of the underlying peak from 142.4 to 145.3°C. Furthermore, we anticipate that the high temperature peak of the PPX coated UHMW-PE filaments close to 152°C overlaps both a possible o–h phase transition signal and the melting of the hexagonal phase. So far our results from the underlying part of the signal coincide with those from the literature. New insights can, however, be obtained from the modulated part of the heat flow rate.

**Table 3** Peak maxima from the underlying signal

| Sample | Peak I $T$/°C | Peak II $T$/°C | Peak III $T$/°C |
|---|---|---|---|
| UHMWE-PE fiber (PE) | 142.4 | 149.6 | 152.0 |
| PPX coated UHMW-PE filament (PPX-45) | 143.5 | – | 151.4 |
| PPX coated UHMW-PE filament (PPX-320) | 145.3 | – | 152.1 |

### *Magnitude signal*

The magnitude of the modulated part of the heat flow rate function, which corresponds to the 'reversing heat flow rate' in the TA concept, (Fig. 5) shows a broad peak from 135 to 152 °C and in addition a small peak on the flank in the melting temperature range of the unconstrained fraction in the orthorhombic phase (corresponding to the 1st peak in the underlying signal). Its maximum in the magnitude signal shifts from 142 to 145°C with PPX coating layer thickness whereas the (small) area under the peak seems to remain nearly unchanged. Obviously, the periodic heat flow signal in the region of this transition at 142°C does not react on the temperature modulation very much, as there is only very little visible in the 'reversing' (magnitude) signal a behaviour, which normally is found if the transition in question is hindered [24]. In other words, the change of transition rate with temperature is that low, that it cannot follow the temperature change in question. For the frequency used, such a behaviour is unusual for melting or other transitions of polymers beside the so-called cold crystallization which takes place far away from the equilibrium and is, for this reason, only weakly influenced by small periodic temperature changes. With respect to the temperature range of the first peak, such a distance to the equilibrium can be excluded in our case. Consequently, a probable explanation of the poor signal relies on a large time constant of that endothermic transition. The transition

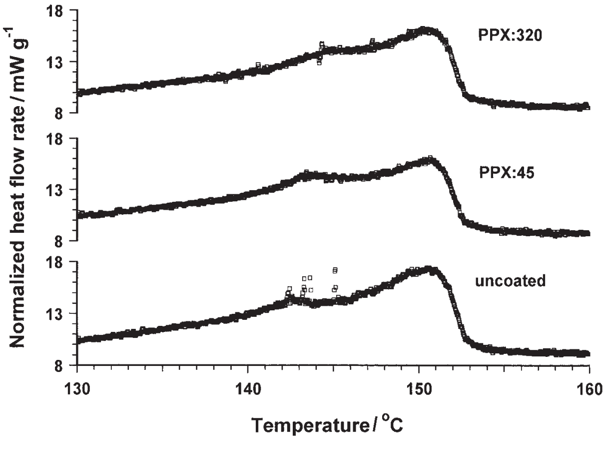

**Fig. 5** Magnitude signal ($\Phi_a$) during melting of the initial gel-spun UHMW-PE fiber, UHMW-PE fiber with a 45 nm PPX coating layer and UHMW-PE fiber with a 320 nm PPX coating layer. Heating rate: 0.1 K min$^{-1}$

can not follow the temperature modulation, consequently the time constant must be larger than the reciprocal angular frequency $1/\omega=5$ s of the modulation for the magnitude to be that low.

The remaining very broad (increasing from 135 to 152°C) peak in the magnitude signal seems to be a normal melting peak of polymers. It coincides with the remaining peak of the underlying curve if we subtract the three peaks at 142.4, 149.6 and 152°C, respectively. Therefore, the broad peak above can be denoted as the melting of the main part of the crystallized fraction and relates to a broad distribution of constraints (stresses). Obviously, the higher the local stresses the higher is the melting temperature of this part of the material. It should be mentioned that it is well known from melting of polymers, that the magnitude signal often starts to deviate from the baseline earlier than it is the case for the underlying (or DSC) signal.

*Phase signal*

The phase shift signal in the melting region is even more difficult to interpret than the magnitude signal is [23, 24]. Nevertheless, the phase shift measurement (Fig. 6) supports the interpretation of the magnitude signal results. Significant is the step-like change in the phase shift at a temperature of about 142°C, which relates to the first peak in the underlying signal, that is the melting of the unconstrained orthorhombic crystal fraction. The step height vanishes with increasing PPX coating layer thickness. This together with the weak peak in the magnitude signal supports the interpretation of a hindered melting, expressed by an increase in the time constant of melting of that orthorhombic crystal fraction with coating layer thickness.

Changes in the phase shift signal before and after the melting region, as observed in Fig. 6 between 130 and 153°C are often caused by changes in heat transport properties either in the sample itself or between sample and sample pan. With respect to the large

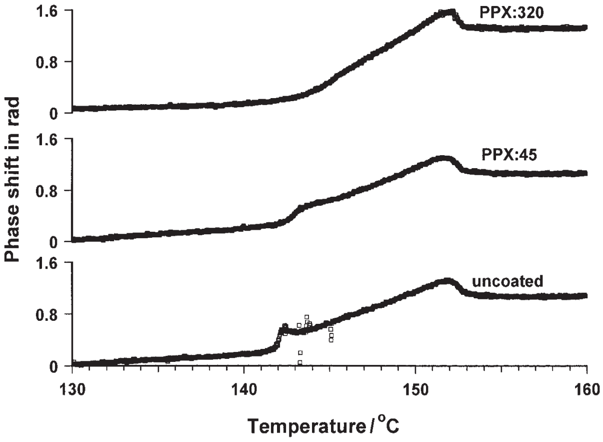

**Fig. 6** Phase shift signal (φ) during melting of the initial gel-spun UHMW-PE fiber, UHMW-PE fiber with a 45 nm PPX coating layer and UHMW-PE fiber with a 320 nm PPX coating layer. Heating rate: 0.1 K min$^{-1}$

phase shift of 0.8 rad and some variation with the coating layer thickness, we may draw the conclusion that the changes of the intrinsic properties are more dominant than eventual contact changes which normally yield not so large phase shifts. It is well-known that stretched PE (fibers) has a much larger heat conductivity in fiber direction than isotropic melt-crystallized PE material (Mergenthaler *et al*. [25]).

## Conclusions

The melting behavior of PPX coated ultradrawn gel-spun UHMW-PE fiber has been investigated by TMDSC with respect to constraints caused by a high temperature stable PPX coating layer. The underlying signal, which corresponds to the normal DSC signal shows for the initial UHMW-PE fiber the melting of the chain-extended fiber fraction of the crystalline orthorhombic phase at 142.4°C, the transition of the orthorhombic to the hexagonal phase of the unmolten constrained fraction at 149.6 and the melting of the hexagonal phase at 152 °C. The PPX coated PE fibers reveal only two endothermic peaks with the maxima at 143.5 and 151.4°C for a PPX layer thickness of 320 nm. The observed shift in the melting peak towards a higher temperature is discussed with respect to constraints due to the PPX coating layer.

The magnitude of the modulated signal (the ‘reversing’ signal) shows only a very weak (in comparison to the underlaying signal) endothermic peak in the region of the melting of the unconstrained orthorhombic crystal fraction. The peak maximum shifts from 142 to 145°C with PPX coating layer thickness. The time constant of this melting process must be larger than the reciprocal angular frequency $1/\omega=5$ s of the modulation to result in such a low magnitude compared to the underlying signal.

The phase shift signal shows a shoulder at about 142°C, which vanishes with increasing PPX coating layer thickness. The transition above belongs to the melting of the unconstrained fraction in the orthorhombic phase.

The magnitude and phase signals characterize the constraints in terms of a hindrance of the melting of the unconstrained fraction of the crystals in the orthorhombic phase. Those processes require time and become even slower with increasing PPX coating layer. Contrary to that, the melting of the fraction still under stress is a broad process, which has been shifted to higher temperatures depending on local forces and their distribution.

For a more detailed analysis about the time constants of melting the frequency and amplitude of the temperature modulation should be varied [26]. Nevertheless, these preliminary results show that TMDSC is a valuable method to get new insights into the effect of constraints on the melting behaviour of highly oriented UHMW-PE fibers.

* * *

Financial support from PTN project-no. 37 PTN4B-3-DP176 is gratefully acknowledged. The authors thank M. Jacobs, DSM Geleen, The Netherlands for fruitful discussions and the supply of the fiber material. A. Spoelstra and A. Saalbrink, TUE Eindhoven is thanked for assistance with the SEM measurements.

## References

1 G. Capaccio and I. Ward, Polym. Eng. Sci., 15 (1975) 2.
2 A. J. Pennings and A. Zwijnenburg, J. Polym. Sci., B17 (1979) 1011.
3 K. Kaji, Y. Ohta, H. Yasuda and M. Murano, Polymer, 22 (1990) 455.
4 Y.-L. Hsieh and J. Ju, J. Appl. Polym. Sci., 53 (1994) 347.
5 B. van Mele and E. Verdonck, Composite Interface, 3 (1995) 83.
6 N. A. J. M. van Aerle and P. J. Lemstra, Polym., 20 (1988) 131.
7 B. Wunderlich and J. Grebowicz, Adv. Polym. Sci., 60/61 (1984) 1.
8 B. Wunderlich, Macromolecular Physics, Vol. 3, Academic Press, New York 1980.
9 D.C. Bassett S. Block and G. J. Piermarini, J. Appl. Phys., 45 (1974) 4146.
10 Y.-L. Hsieh and X.-P. Hu, J. Polym. Sci. B: Polym. Phys., 35 (1997) 623.
11 J. Smook and J. Pennings, Colloid Polym. Sci., 262 (1984) 712.
12 Private communication.
13 W. F. Gorham, J. Polym. Sci., A1 (1966) 3030.
14 Encyclopedia of Polymer Sci. and Engineering, Wiley, New York, 17 (1989) 990.
15 R. Iwamoto, R. C., Bopp and B. Wunderlich, J. Polym. Sci.: Polym. Phys. Ed., 13 (1975) 1925.
16 S. Isoda, A. Kawaguchi and K.-I. Katayama, J. Polym. Sci.: Polym. Phys. Ed., 22 (1984) 669.
17 H. van der Werff and A. J. Pennings, Polym. Bull., 19 (1988) 587.
18 H. van der Werff and A. J. Pennings, Colloid and Polym. Sci., 269 (1991) 747.
19 U. Göschel and H. Walter, Langmuir, in press.
20 Product information from DSM, Geleen, The Netherlands.
21 G.W.H. Höhne, Thermochim. Acta, 303/304 (1997) 209.
22 S. Isoda, Polymer, 25 (1984) 615.
23 G. W.H. Höhne, Thermochim. Acta, 330 (1999) 45.
24 G. W. H. Höhne, Thermochim. Acta, 330 (1999) 93.
25 D. B. Mergenthaler, M. Pietralla, S. Roy and H.-G. Kilian, Macromolecules, 25 (1992) 3500.
26 To be published elsewhere.